Optimising 3D coal seismic imaging with pre-stack depth migration

Xiaodong Lu
Velseis Pty Ltd
83 Jijaws St Sumner QLD 4074
xlu@velseis.com

Alan Meulenbroek
Velseis Pty Ltd
83 Jijaws St Sumner QLD 4074
alanm@velseis.com

Karel Driml
Velseis Pty Ltd
83 Jijaws St Sumner QLD 4074
kdriml@velseis.com

SUMMARY

Pre-stack depth migration (PSDM) is applied to a 3D seismic survey from the Bowen Basin in QLD to improve imaging of shallow coal-seams which suffer from poor signal-to-noise caused by poor statics and velocities.

Two different velocity fields are used as initial velocity models. The first is the PSTM velocity field and the second is created based on imaging reflections from the base of weathering.

Final seismic images obtained after PSDM velocity updates indicate that the second velocity model is superior in imaging the poor data area and is more representative of depths observed in borehole data. Both initial models yield superior imaging results compared to the time-processing results.

Key words: PSDM, imaging, coal.

INTRODUCTION

High-resolution imaging of shallow target coal seams relies on the derivation of precise static solutions and velocity models. Where challenging geological conditions exist, precision in these models can be lost, resulting in poor imaging.

Pre-stack depth migration (PSDM) is routinely used in the oil and gas industry for improved imaging, however, it is not exploited to the same extent in the coal industry. This paper discusses the application of PSDM to a 3D Vibroseis dataset from a mine in the Bowen Basin which suffers from poor imaging.

APPLICATION TO 3D COAL DATA

The seismic data used for this case-study are from the Bowen Basin in central QLD. It is a 3D Vibroseis survey acquired in 2018 and processed by Velseis in 2019. The data quality varies significantly across the survey area. The poor data quality area is caused by a combination of very thick weathering and challenging surface conditions which adversely affected source coupling.

Figure 1 shows a raw shot record (with AGC applied) from an area of good data quality. The ground-roll (yellow), first-breaks (red) and target reflector (green) are annotated.

Figure 2 shows a raw shot record (with AGC applied) from the poor-quality area. The yellow and red again show the ground-roll and first-breaks. No reflection energy can be identified on this shot record. Note that the dominant frequency of Figure 2 is much lower than Figure 1. This is caused by a combination of poor source-coupling and very deep (~80m) weathering in this area.

The data were processed using a flow designed to maximise the signal-to-noise ratio of the target reflector. This included refraction statics, velocity picking, random and coherent noise attenuation and spectral enhancement. The data were migrated using conventional PSTM.

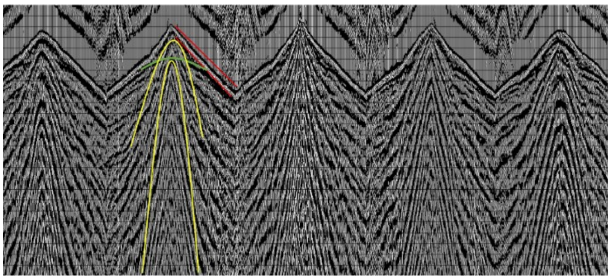

Figure 1. AGC 3D shot record from area of good data quality. Ground-roll energy is yellow, first-break energy is red and target reflector is green. Vertical scale is time.

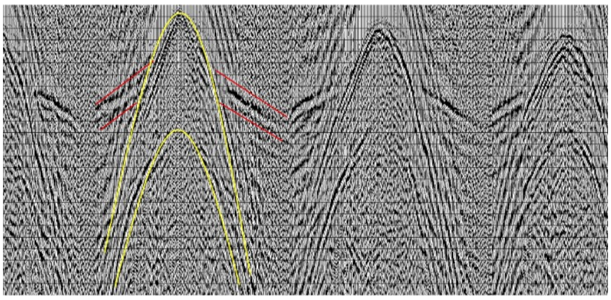

Figure 2. AGC 3D shot record from area of poor data quality. Ground-roll energy is yellow, first-break energy is red. No reflection energy can be identified. Vertical scale is time.

A line taken from the PSTM stacked volume is shown in Figure 3. This image has been depth-converted using the PSTM velocities. In this and in all subsequent stacks, the yellow line represents the surface elevation. The variability in data quality is clearly evident along the line. On the right half, the target coal-seam has been imaged well and structure within the coal-seam is well resolved. In contrast, the same target coal-seam is poorly imaged on the left with areas of little or no coherency in the data. The poor image is a result of inadequate static corrections due to the relatively poor first-breaks observed in Figure 2. Note also that some of the data appears above the surface. This is also indicative of a poor statics solution.

On the far left of the line, the target coal reflector is imaged relatively well, however, there does appear to be an anticline present. While this may be geologically plausible, given the challenging data quality in this area, it is also possibly an artificial pull-up caused by incorrect velocities. Pull-ups like this can appear in time images (e.g. in the presence of dykes), however, in the depth domain, a velocity model with sufficient precision should resolve this ambiguity.

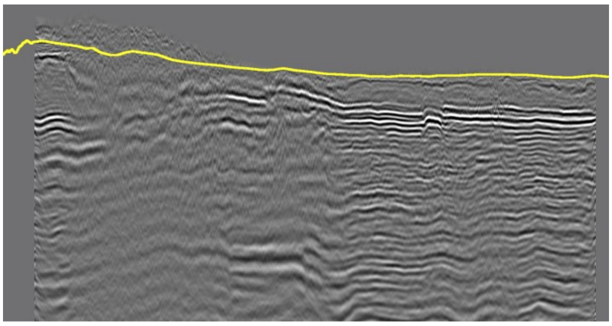

Figure 3. PSTM stack converted to depth using PSTM velocities. The yellow line is the surface elevation. Horizontal distance is approximately 1.6km and depth range is 0-800m depth from seismic datum.

Overlaying the interval velocity field onto the stack (Figure 4) illustrates the relationship between the two. Broadly speaking, the top-of-coal reflector can be correlated to the change from dark green to lime green. The exception to this is the area where the target coal reflector disappears altogether, suggesting the velocity may not be optimised in this area. The lateral blocky nature of the velocity field is a function of manual NMO velocity picking which is performed at regular intervals.

The poor correlation between geology and velocity model in the poor data zone suggests that there is room for significant improvement. This is achieved using PSDM. An important consideration is the initial velocity model. The first approach utilises the PSTM velocity field as the initial model.

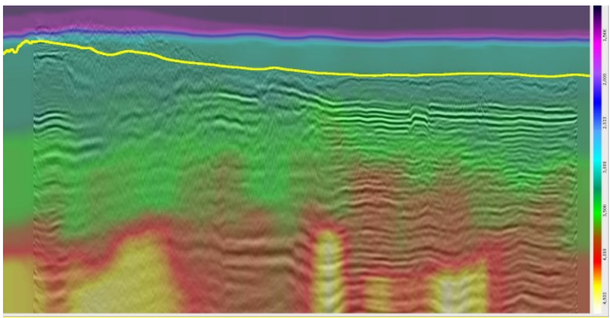

Figure 4. PSTM stack with PSTM interval velocity field overlay. Vertical scale is depth. Velocity range is from 1100m/s (dark purple) to 4600m/s (yellow/white). The yellow line is the smoothed surface elevation. Horizontal distance is approximately 1.6km and depth range is 0-800m depth from seismic datum.

PSTM INITIAL MODEL

A smoothed version of the velocity field shown in Figure 4 was used as an initial model for PSDM. The velocity field was iteratively updated 6 times until it converged to a solution. The resulting stack is shown in Figure 5 and the stack with the final interval velocity field overlay is shown in Figure 6.

The image in Figure 5 has obvious improvements over Figure 3. The target coal reflector can now be traced through the poor-data zone. Importantly, the PSDM image in the good data-quality zone has not been degraded relative to the PSTM image. In contrast, the imaging of the faults has improved on the PSDM image. At the far-left end of the line, the anticlinal structure present in Figure 3 has been flattened.

Comparison between the velocity fields in Figure 4 and Figure 6 indicates that the final PSDM velocity field is more representative of the geology than the initial model. The seismic velocity above the target coal seams (consolidated sandstone/siltstone) is approximately 3200-3500m/s (green) whereas the velocity through the coal package ranges from 2200m/s to 2700m/s (dark and light blue). These velocities are consistent with known P-wave seismic velocities in these rock types in the Bowen Basin. The relatively slow velocity in the middle of the line (dark blue) is likely caused by fracturing of the rock in the faulted zone.

While the latest velocity model results in a vast improvement over the PSTM velocity model, there are indications in Figure 6 that further enhancements can be pursued. The main indication is the presence of the large red/yellow zone in the centre of the line in the deeper section. These colours represent velocities of ~4500m/s. A P-wave velocity of 4500m/s is not typical of the sedimentary stratigraphy observed in the Bowen Basin. These velocities are generally reserved for carbonate sedimentary rocks or igneous rocks (e.g. Bourbie et al., 1987) neither of which are present here. The effect of these high velocities, and the deeper velocity variation in general, can be seen in the geometry of the deeper reflectors. Faster velocities have pushed the data deeper and slower velocities have pulled the data shallower. The resulting syncline/anticline is a direct result of these velocity variations.

This deep high velocity zone is likely to be an artefact, created by the algorithm in response to the initial model (The velocity update has converged to a local, rather than a global, minimum.) An initial velocity model which is more geologically realistic is more likely to converge to the true velocity than one that is less realistic. This improved velocity model is created using prior information external to the initial PSTM velocity field.

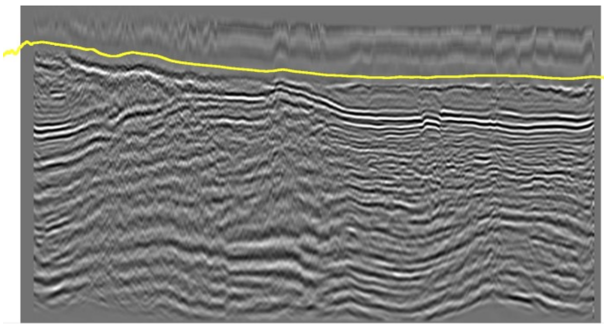

Figure 5. PSDM stack where initial model does not include the weathering model. The yellow line is the smoothed surface elevation. Horizontal distance is approximately 1.6km and depth range is 0-800m depth from seismic datum.

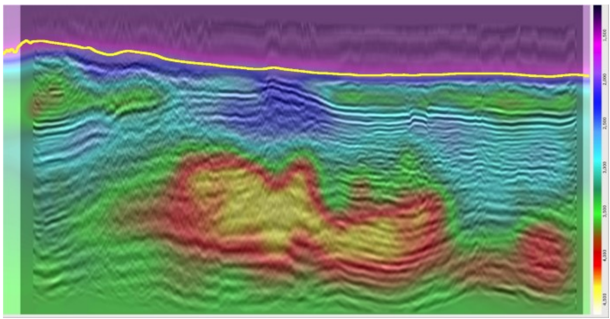

Figure 6. PSDM stack in Figure 5 with final interval velocity overlayed. The yellow line is the smoothed surface elevation. Horizontal distance is approximately 1.6km and depth range is 0-800m depth from seismic datum.

IMPROVED INITIAL MODEL

The improved initial model is built based on imaging reflections from the base of weathering. The approach of imaging the base of weathering using PSDM implemented here is broadly the same as the workflow outlined in Yilmaz (2013). The aim is to image reflections, rather than refractions, arising from the base of weathering. The strength/sharpness of these reflections on a stacked image is related to the velocity of the near-surface.

The improved initial model workflow is as follows:

1. Offset limit the data. Because the target in this context is the base of weathering reflection event, the data used for PSDM can be offset-limited so that only near-offsets which record this event are used.
2. Apply all high-frequency statics. Long-period statics (weathering corrections) are not applied. If refraction statics are applied, information about the structure of the weathering layer is lost.
3. Adjust data to the migration-surface datum. The offset-limited gathers are adjusted to a datum which is a smoothed version of the topography (migration surface). The gathers are converted to depth using the most recent interval velocity model derived from NMO velocity picking.
4. Velocity scan. Perform PSDM using a range of constant velocity models. The velocities which result in the best stacked images in different areas are picked, interpolated and smoothed to form a 3D velocity model of the weathering layer.
5. Build full model. Incorporate this near-surface velocity model with known constraints deeper in the section to produce an initial velocity model.

For these data, the constant velocity scans were performed using values of 1200m/s to 1800m/s in increments of 100m/s.

Figure 7 shows an example stack in which the base-of-weathering reflector has been imaged along the full length of the line. Note the seismic section has a limited depth extent because only the near-offsets have been used. The variation in depth to the base of weathering can clearly be seen. On the right side, the shallow base of weathering results in a sharp image whereas the deeper reflection and poor surface conditions on the left results in a broader wavelet. The amplitude of the event varies significantly along the line. While the shallower reflector is sharper, there are fewer traces which sample this event, hence the lower amplitude.

The velocity model used to create the image in Figure 7 is shown in Figure 8. The weathering velocity varies laterally in accordance with the stack response shown in Figure 7. On the right, a relatively slower weathering velocity (~1400m/s) has been picked compared to the areas on the left (~1600m/s – 1800m/s). While these differences in velocity appear minimal, in the context of the near-surface, the differences represent a significant proportion of the true velocity. Additionally, in the near-surface, the propagation distances are relatively short meaning small differences in velocity can have a large effect on event timing and imaging.

In contrast to the PSTM initial model (Figure 4) the velocity below the base of weathering has been set to a constant 3500m/s. In the absence of deeper boreholes, this is a more geologically consistent initial velocity which allows the optimisation scheme a greater chance of converging to a solution that is more representative of the true velocity field. A smooth velocity gradient between the weathering and sub-weathering has been created which is better suited to the migration algorithm than if a sharp velocity boundary was imposed.

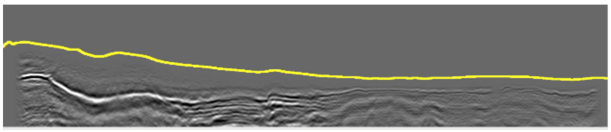

Figure 7. Base of weathering reflector imaged using starting model shown in Figure 8. Yellow line is the surface elevation. Horizontal distance is approximately 1.6km and depth range is 0-300m depth from seismic datum.

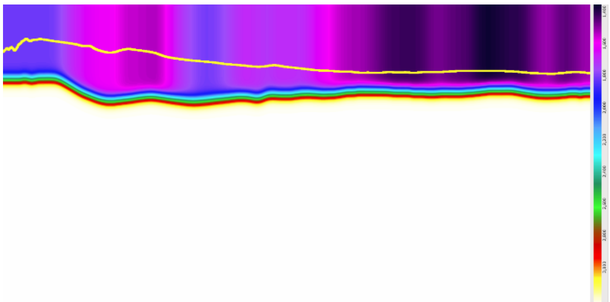

Figure 8. Initial velocity model used for PSDM. Velocity ranges from 1400m/s (purple) to 3500m/s (white). Yellow line is the surface elevation. Horizontal distance is approximately 1.6km and depth range is 0-800m depth from seismic datum.

The velocity was iteratively updated 6 times until it converged to a solution. The resulting stack is shown in Figure 9 and the stack with the final interval velocity field overlay is shown in Figure 10.

The region of low velocity related to the faulted zone in the middle of the line seen in Figure 6 is also present in Figure 9. This indicates that the different starting models have converged to a similar velocity structure in this region. Relatively high velocities (>4000m/s) are present in the shallow section of Figure 10 but this is far less extensive than seen in Figure 6. Borehole logs in this area do not suggest the presence of rocks with seismic velocities in this range. This may be caused by non-uniqueness related to the slower weathering velocities present in the initial model. Given that the focus of this study is the shallow targets, and with an absence of deep borehole data, any deeper velocity value >3600m/s has been clipped to 3600m/s for stacking. Although not the focus of this imaging exercise, the geometry of the deep reflectors in Figure 9 appear more realistic than those in Figure 5 albeit with a slightly poorer stack response.

The similarity in the broad-scale structure of the final velocity models obtained from different initial models means that the resulting stacks (c.f. Figure 9 and Figure 5) are also very similar. Overall, however, the resolution and event continuity at the target reflectors are both superior in Figure 9. The main areas of improvement are where the coal-seam is shallowest in the centre of the line as well as the structure resolution on the left end of the line. The noise above the surface elevation is caused by the AGC operator.

Another subtle but very important improvement is that the depth of the events is now more realistic. Although the shallow structure of the final velocity profiles is similar, the velocity values are different (Figure 6 and Figure 10 are plotted on the same scale for comparison). This affects the depth at which the events are imaged. Subsequent investigations outside the scope of this paper have concluded that the depths presented in Figure 9 are more representative of the true depths measured directly from boreholes.

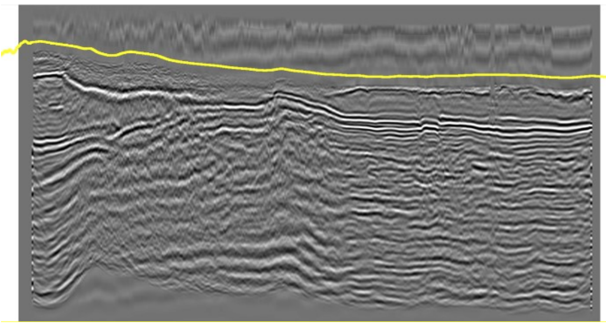

Figure 9. Final PSDM stack derived where weathering velocity incorporated into initial velocity model. Horizontal distance is approximately 1.6km and depth range is 0-800m depth from seismic datum.

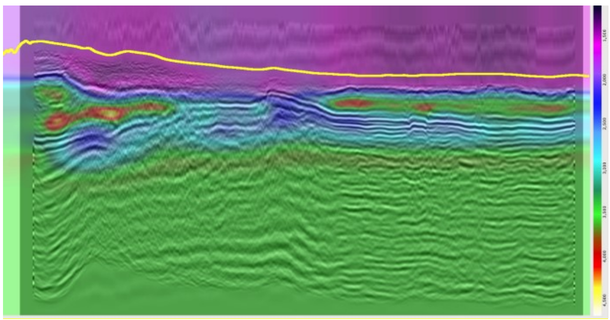

Figure 10. PSDM stack from Figure 9 with final interval velocity overlayed. Horizontal distance is approximately 1.6km and depth range is 0-800m depth from seismic datum.

CONCLUSIONS

The application of PSDM to this coal dataset from the Bowen Basin has vastly improved the image produced from routine time processing. The target coal horizon can now be identified and picked in the area which was effectively uninterpretable on the original time-processed section. This improves geological interpretability, resource estimation and safety factors related to the identification of target coal seams and characterisation of structures which may affect those seams.

The variation in signal-to-noise in this dataset was advantageous for PSDM testing because results could be analysed in both poor and good data areas. While the main effort was focussed in the poor data area, subtle but valuable improvements were also obtained in the good data area. This suggests that PSDM could be used not only to improve poor seismic imaging, but to further improve areas where resolution needs to be maximised, e.g. near faults and structures.

While the workflow presented here for imaging the base of weathering (based on Yilmaz, 2013) has been used to improve imaging at the final PSDM stage of processing, Yilmaz originally presented this methodology for calculating a statics solution at the very beginning of the processing sequence. I.e. it is presented as an alternative to traditional statics calculation methods. While this was not done here, the relevant information (surface elevation, depth to base of weathering, weathering velocity) is made available by this workflow to do this if so desired.

PSDM is routinely used in the oil and gas industry to improve subsurface imaging. This paper has demonstrated that PSDM can also be successfully applied in the coal context. There are many areas in the Bowen Basin which suffer from poor seismic imaging caused by various geological factors (e.g. tertiary cover or basalt). It is likely that many of these areas could benefit from the application of PSDM.

ACKNOWLEDGMENTS

The authors would like to thank the host mine for permission to present the data in this paper, and John Walker, of Walker Geophysical for his technical input.

REFERENCES

Bourbie, T., Coussy, O., Zinszner, B., 1987, Acoustics of porous media. Editions Technip, Paris.

Yilmaz, O, 2013, An image-based effective-medium modelling of near-surface anomalies: *The Leading Edge*, 32, pp394-401.